AIP | Review of Scientific Instruments

Long-working-distance microscopic imaging in a turbid medium by use of an ultrafast optical Kerr gate

Yuhu Ren, Wenjiang Tan, Yipeng Zheng, Xiaojing Liu, and Junyi Tong

Citation: Review of Scientific Instruments **87**, 063708 (2016); doi: 10.1063/1.4953763
View online: http://dx.doi.org/10.1063/1.4953763
View Table of Contents: http://scitation.aip.org/content/aip/journal/rsi/87/6?ver=pdfcov
Published by the AIP Publishing

Long-working-distance microscopic imaging in a turbid medium by use of an ultrafast optical Kerr gate

Yuhu Ren,[1] Wenjiang Tan,[1,a)] Yipeng Zheng,[1] Xiaojing Liu,[1] and Junyi Tong[2]
[1]*Key Laboratory for Physical Electronics and Devices of the Ministry of Education & Shaanxi Key Lab of Information Photonic Technique, Collaborative Innovation Center of Suzhou Nano Science and Technology, School of Electronics & Information Engineering, Xi'an Jiaotong University, Xianning-xilu 28, Xi'an 710049, China*
[2]*Departments of Applied Physics, Xi'an University of Technology, Xi'an 710048, China*

(Received 19 February 2016; accepted 31 May 2016; published online 15 June 2016)

We demonstrate a long-working-distance microscopic imaging of hidden objects in a turbid medium by use of an ultrafast optical Kerr gate (OKG). The results show that the working distance and the spatial resolution of the long-working-distance microscopic imaging system have been increased simultaneously compared with those of the conventional 4f OKG imaging systems. A compound lens consisting of a long-focus achromatic doublet and a microscope objective is used to increase the long working distance and ensure the sufficient spatial resolution. The microscopic OKG imaging system with a working distance of 245 mm and a maximal spatial resolution of approximately 7 μm has been performed. *Published by AIP Publishing.* [http://dx.doi.org/10.1063/1.4953763]

I. INTRODUCTION

Optical imaging of hidden objects in highly scattering media has wide applications in many areas such as biological tissues,[1] fogs,[2] or aerated sprays.[3,4] The image quality is often degraded because of the noise that arises from the multiple light scattering. Generally, the photons transmitted from a turbid medium are split into three components, the ballistic, the snake, and the diffuse components.[5] The ballistic photons migrated through the turbid medium in a straight line and the snake photons undergo along quasi-straight-line paths. But the diffuse photons participate in more interaction events and traverse a more circuitous path through the medium. The difference in optical path length of these three components leads to the temporal spreading of a light pulse propagating in a turbid medium.

Several techniques have been introduced to sense objects hidden in turbid media.[6–8] A feasible way is detecting the ballistic and the snake components but removing the diffuse component, which can be accomplished by a time-gated technique. Several nonlinear optics effects, such as the degenerate four wave mixing,[9] the second harmonic generation,[10] or the optical Kerr effect[11–13] have been used to realize the ultrafast time gate. Among the available time gated imaging techniques, the optical Kerr gated (OKG) imaging based on the optical Kerr effect has been used widely due to its advantages, such as no need for satisfaction of the phase-matching condition or the capability to acquire a time-sliced true 2D spatial image for both incoherent and coherent optical signals.[14]

It is well-known that optical microscopy plays an important role in examining small features in the field of physical, chemical, and biological systems.[15] The optical microscopic imaging through highly scattering media such as the confocal microscopy[16] and optical coherence microscopy[17] has been widely used in science and industry. However, most of the usual microscopic techniques for scattering media are limited to image the slow-moving objects and even the immovable objects. On the contrary, some previous researches showed that OKG microscopy is capable of acquiring wide field fluorescence images with femtosecond time resolution,[18] which indicated OKG microscopy being also a feasible way to image the fast-moving tiny objects hidden in turbid media. However, many conventional OKG microscopic systems have a relatively short working distance less than 50 mm due to the restriction of a microscope objective.[19] The short working distance limits the application of OKG microscopic imaging in which it is necessary to place a microscopic objective far from the object. For example, to study the tiny structure such as small droplets (~10 μm) in the near field of a high-speed strong scattering fuel spray, the working distance of the imaging system should be more than 200 mm to avoid the optical elements contaminated or damaged. Therefore, it is helpful to develop a long-working-distance OKG microscopic imaging system to image fast-moving tiny objects hidden in turbid media.

In this paper, we demonstrate a long-working-distance OKG microscopic imaging through a turbid medium. A sequence of microscopic images of a test chart hidden behind a turbid medium is obtained. Since the 4f OKG imaging systems are widely used in imaging objects hidden in turbid media, we compare the working distance and image resolution of the long-working-distance OKG microscopic imaging system with those of the conventional 4f OKG imaging systems.[20,21] The results show that the working distance and imaging resolution can be increased simultaneously in the long-working-distance OKG microscopic imaging system.

II. EXPERIMENTAL SETUP

The experimental optical setups are shown in Figure 1. The laser beam from a Ti:sapphire laser providing 800 nm,

a)Electronic mail: tanwenjiang@mail.xjtu.edu.cn

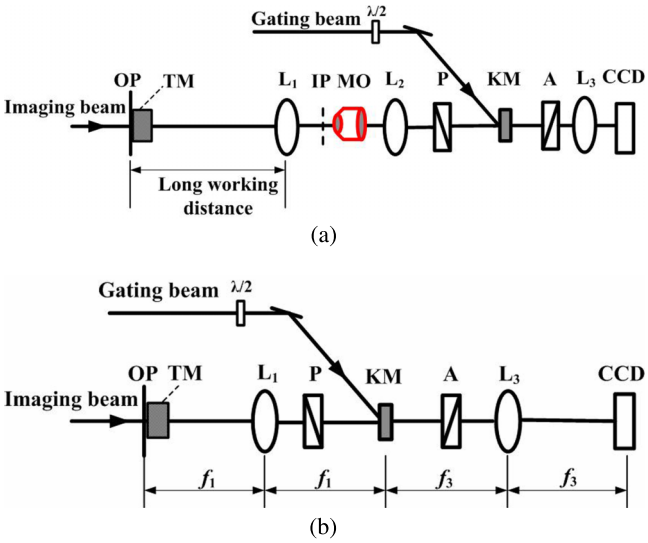

FIG. 1. (a) Long-working-distance OKG microscopic imaging setup. (b) 4f OKG imaging setup. OP: objective plane; TM: turbid medium; IP: image plane; L: lens; MO: microscope objective; λ/2: half-wave plate; P: polarizer; A: analyzer; KM: Kerr medium; CCD: charge coupled device; f_1, f_3 focal lengths for the lens L_1 and L_3, respectively.

50 fs pulses at a repetition rate of 1 kHz was split into a gating beam centered at 780 nm and an imaging beam centered at 800 nm by a short pass filter (SPF) (not shown in the figure). The polarization of the gating beam was first linearly polarized at 45° with respect to the polarization of the imaging beam for optimal efficiency using a half-wave (λ/2) plate. The gating beam was focused into the Kerr medium of CS_2 filled in a 5 mm quartz cell. The main difference between the two optical setups was in how the imaging pulse was introduced to the charge coupled device (CCD) camera. A US Air Force resolution test chart with 1.41-line-pair/mm was used as the target to be imaged. The target was placed behind a turbid medium. The turbid medium used in the experiment was composed of a polystyrene microsphere solution contained in a cubic cell with inside dimensions of 50 mm × 50 mm × 10 mm. The thickness of the cell along the optical axis was 10 mm. The diameter of the polystyrene microspheres was 3.13 μm. The absorption of the turbid medium was low enough to be ignored. The value of the optical density (OD) of the sample was OD = 5.2.

In Fig. 1(a), we show the schematic of the long-working-distance OKG microscopic imaging system. The working distance for this imaging system was 245 mm. In this imaging system, the object was first imaged by the first achromatic doublet (L_1) with focal length of f_1 = 150 mm onto the image plane. Then the image was magnified by the microscope objective [10× numerical aperture (NA) = 0.25, Nikon] and the second lens (L_2) with focal length of f_2 = 100 mm. The third lens (L_3) with focal length of f_3 = 150 mm was used to adjust the image position and magnification with respect to the CCD. In this setup, the imaging pulse was spatially overlapped with the gating pulse in the Kerr medium which was placed at the focal plane of a compound lens consisting of the microscope objective and lens (L_2). The arrangement of the OKG in the long-working-distance microscopic imaging is the same as Ref. 22.

However, in the conventional 4f OKG imaging configuration shown in Fig. 1(b), the object plane was placed one focal length in front of the achromatic doublet (L_1) and the image plane was located one focal length behind the second lens (L_3). The OKG was placed between the two lenses with the CS_2 cell slightly behind the focal point of the collecting lens to avoid focusing directly into the CS_2. In the two setups, when the two pulses were spatially and temporally overlapped, the imaging pulse polarization was rotated due to the birefringence of the Kerr media induced by the gating pulse. Then the early part of the imaging pulse passed through the analyzer, which was detected by the CCD camera.

III. RESULTS AND DISCUSSION

The images of the test chart hidden behind a polystyrene microsphere sample are demonstrated by use of long-working-distance OKG microscopic imaging and 4f OKG imaging, respectively. In Fig. 2(a), we show direct microscopic imaging for the sample filled with deionized water as the reference image. In Fig. 2(b), we show direct microscopic imaging for the sample filled with the polystyrene microsphere turbid medium. A slightly recognizable image is observed, which is affected by the scattered photons. In Figs. 2(c) and 2(d), we show the long-working-distance OKG microscopic imaging and 4f OKG imaging, respectively, for the polystyrene microsphere turbid medium. As shown in Fig. 2(c), the long-working-distance OKG microscopic imaging provides a better image quality than that of Fig. 2(b). The long-working-distance OKG microscopic imaging improves image visibility and enhances the contrast between the target and its background. The improved image

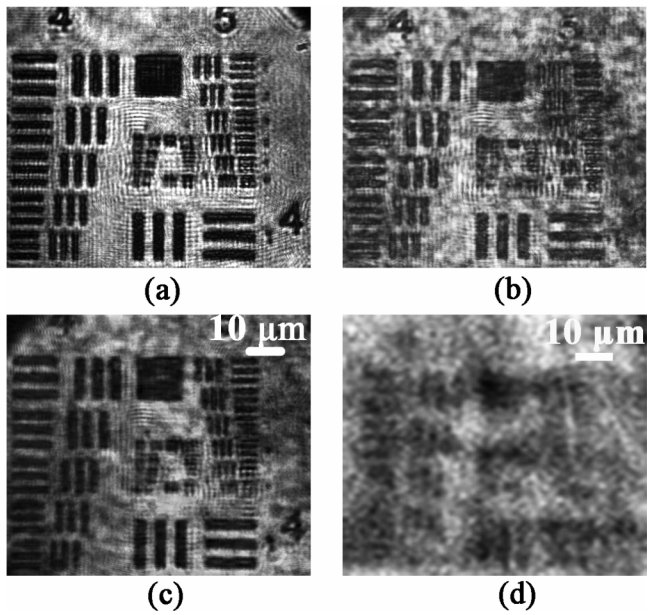

FIG. 2. Images of the test chart behind water and the polystyrene microsphere turbid medium. (a) Reference image. (b) No time gate (standard transillumination). (c) Long-working-distance OKG image for the polystyrene microsphere turbid medium. (d) 4f OKG image for the polystyrene microsphere turbid medium.

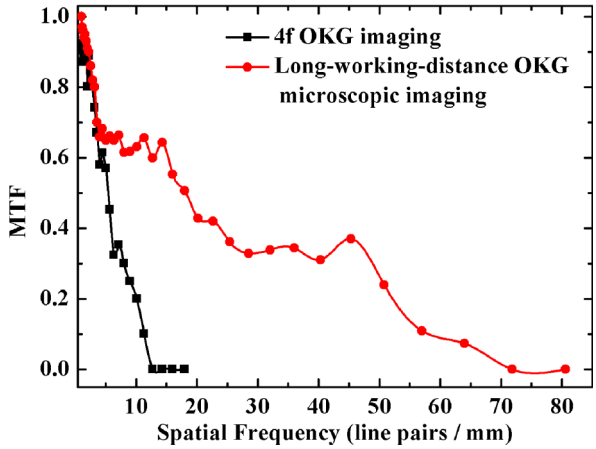

FIG. 3. Comparison of the MTF of the long-working-distance OKG microscopic imaging system and the 4f OKG imaging system.

visibility and enhanced contrast can be attributed to the selection of the ballistic photons, with most of the scattered photons filtered out by the OKG. However, for the 4f OKG imaging shown in Fig. 2(d), the imaging resolution decreases obviously compared to that of the long-working-distance OKG microscopic imaging.

To quantitatively evaluate the performance of the long-working-distance OKG microscopic imaging system and the conventional 4f OKG imaging system, we further measured the modulation transfer function (MTF) of the two systems. The MTF is given by $MTF(f) = C(f)/C_0(f)$, where the image contrast is defined as $C(f) = (I_{max} - I_{min})/(I_{max} + I_{min})$. Further, $C_0(f)$ denotes the modulation of the object, and f is the spatial frequency. The image contrast is calculated using the average light intensity retrieved from the dark region (I_{min}) and the average light retrieved from the unshadowed region (I_{max}) of the test chart. From Fig. 3, we can see that the spatial resolution of the long-working-distance OKG microscopic imaging system is higher than that of the 4f OKG imaging system. For the long-working-distance OKG microscopic imaging, the cutoff spatial frequency is 71.8 line pairs per millimeter (lp/mm) with a corresponding resolved object size 6.96 μm in our experiments. However, for the 4f OKG imaging system, the cutoff spatial frequency is 12.7 lp/mm with a corresponding resolved object size 39.37 μm. Compared with the 4f OKG imaging, the long-working-distance OKG microscopic imaging has a higher image spatial resolution. The abruptly decreased image spatial resolution of 4f OKG imaging could be attributed to the lower numerical aperture (NA) and spatial-filtering effect of the imaging system. The spatial-filtering effect is due to the transient soft aperture in the Kerr material, which arises from the finite spot size of the gating beam. The transient soft aperture acts as a low-pass filter, which enables the low spatial frequency components of the imaged object pass but removes the high spatial frequency components. The low spatial frequency components are at the center of the Fourier plane of the compound lens consisting of the microscope objective and lens (L_2), while the high spatial frequency components are in the peripheral area of the Fourier plane. However, the arrangement of the long-working-distance OKG microscopic imaging system could increase the numerical aperture using the microscope objective and reduce the spatial-filtering effect by rotating the analyzer by a few degrees.[23] The ripples in the MTF arise from the aberrations in the imaging systems and the nonuniform of the imaging beams.[24]

The different imaging resolutions of the long-working-distance OKG microscopic imaging system and the conventional 4f OKG imaging system can be explained as follows. According to the Rayleigh criterion, the highest resolution of an imaging system depends on the numerical aperture (NA) of the imaging system and the wavelength of illumination light.[25] For the 4f OKG imaging system, the highest imaging resolution is $r_0 = 0.61\lambda/NA = 1.22\lambda f/D$, where f is the focal length of the achromatic doublet (L_1), λ is the wave length of the imaging beam, and D is the size of the aperture stop of the imaging system. For the long-working-distance OKG microscopic imaging system, the highest imaging resolution is $r_0 = 0.61\lambda/NA = 1.22\lambda L/D/A$, where L is the distance between the aperture stop and the image plane, and A is the magnification of the microscopic imaging system. In our experiment setups, the stop sizes of the 4f OKG imaging system and long-working-distance OKG microscopic imaging system are approximately 4 mm and 13 mm, respectively. The distance L of the long-working-distance OKG microscopic imaging system is approximately 640 mm. The magnification A of the microscopic imaging system is about 10. Hence, in theory, the image spatial resolutions of the long-working-distance OKG microscopic imaging system and the 4f OKG imaging system are about 4.5 μm and 36.6 μm, respectively. The highest imaging resolutions of the two imaging systems in our experiment are slightly lower than those predicted by the Rayleigh criterion. This phenomenon can be attributed to the aberrations of the imaging systems.[26]

Further, we compare the working distance and image resolution obtained in this paper with those reported in earlier literature. The results are listed in Table I. From Table I, we see that the 4f OKG imaging systems have moderate image spatial resolution and working distance compared with the long-working-distance OKG microscopic imaging system. Further, the microscopic OKG imaging system with a working distance of 245 mm and a maximal lateral resolution of approximately 7 μm has been performed. Compared with the conventional 4f OKG imaging systems, the microscopic OKG imaging system in our paper can improve the imaging resolution and increase the working-distance simultaneously. We can also see that the working-distance can be increased, but the highest resolved imaging resolution will seriously decrease in the single lens imaging system from Table I.

TABLE I. Comparison of the working distance and image resolution obtained in this paper with those in earlier literature.

Optical configuration	Working distance (mm)	Resolution (μm)
4f-system[27]	200	>10
4f-system[28]	150	>15
Single-lens-system[29]	>500	>50
Microscopic-system (in this paper)	245	~7

IV. CONCLUSION

In conclusion, we have demonstrated a long-working-distance microscopic imaging through a turbid medium by use of an OKG. The results show that the working distance and the spatial resolution of the long-working-distance microscopic imaging system can be increased simultaneously compared with those of the 4f OKG imaging. A compound lens consisting of a long-focus achromatic doublet and a microscope object is used to increase the long working distance and ensure the sufficient spatial resolution. The microscopic OKG imaging system with a working distance of 245 mm and a maximal spatial resolution of approximately 7 μm has been performed. The long-working-distance OKG microscopic imaging technique is potentially applicable to obtain the images of the structure in a real spray.

ACKNOWLEDGMENTS

The authors gratefully acknowledge the financial support for this work provided by the National Natural Science Foundation of China under Grant Nos. 61235003, 61427816, 61205129, and 61308036, Natural Science Basic Research Plan in Shaanxi Province of China (Program No. 2014JQ8363), in part by the Collaborative Innovation Center of Suzhou Nano Science and Technology and in part by the Open Found of State Key Laboratory on Integrated Optoelectronics, under Grant No. IOSKL2015KF24.

[1]R. Liao, N. Zeng, X. Y. Jiang, D. Z. Li, and T. L. Yun, J. Biomed. Opt. **15**, 036014 (2010).
[2]J. Fade, S. Panigrahi, A. Carré, L. Frein, C. Hamel, F. Bretenaker, H. Ramachandran, and M. Alouini, Appl. Opt. **53**, 3854 (2014).
[3]D. Sedarsky, J. Gord, C. Carter, T. Meyer, and M. Linne, Opt. Lett. **34**, 2748 (2009).
[4]S. P. Duran, J. M. Porter, and T. E. Parker, Appl. Opt. **54**, 1743 (2015).
[5]L. Wang, P. P. Ho, C. Liu, G. Zhang, and R. R. Alfano, Science **253**, 769 (1991).
[6]W. Chu, H. L. Li, J. L. Ni, B. Zeng, J. P. Yao, H. S. Zhang, G. H. Li, H. L. Xu, and Y. Cheng, Appl. Phys. Lett. **104**, 091106 (2014).
[7]H. L. Li, H. L. Xu, B. S. Yang, Q. D. Chen, T. Zhang, and H. B. Sun, Opt. Lett. **38**, 1250 (2013).
[8]H. L. Xu and S. L. Chin, Sensors **11**, 32 (2011).
[9]A. D. Sappey, Appl. Opt. **33**, 8346 (1994).
[10]S. Idlahcen, C. Rozé, L. Méès, T. Girasole, and J. B. Blaisot, Exp. Fluids **52**, 289 (2012).
[11]R. Nakamura and Y. Kanematsu, Rev. Sci. Instrum. **75**, 636 (2004).
[12]L. Yan, J. Yue, J. Si, and X. Hou, Opt. Express **16**, 12069 (2008).
[13]J. Yue, L. Yan, J. Si, F. Chen, Q. Yang, X. Hou, G. Qian, and J. Guo, Opt. Commun. **282**, 1448 (2009).
[14]B. L. Yu, A. B. Bykov, T. Qiu, P. P. Ho, R. R. Alfano, and N. Borrelli, Opt. Commun. **215**, 407 (2003).
[15]R. L. Sandberg, A. Paul, D. A. Raymondson, S. Hädrich, D. M. Gaudiosi, J. Holtsnider, R. I. Tobey, O. Cohen, M. M. Murnane, and H. Kaptern, Phys. Rev. Lett. **99**, 098103 (2007).
[16]P. Guitera, G. Pellacani, K. A. Crotty, R. A. Scolyer, L. X. L. Li, S. Bassoli, and S. W. Menzies, J. Invest. Dermatol. **130**, 2080 (2010).
[17]I. Grulkowski, J. J. Liu, B. Potsaid, V. Jayaraman, J. Jiang, J. G. Fujimoto, and A. E. Cable, Opt. Lett. **38**, 673 (2013).
[18]M. Seo, S. Boubanga-Tombet, J. Yoo, Z. Ku, A. V. Gin, S. T. Picraux, S. R. J. Brueck, A. J. Taylor, and R. P. Prasankumar, Opt. Express **21**, 8763 (2013).
[19]M. B. Sinclair, M. P. de Boer, and A. D. Corwin, Appl. Opt. **44**, 7714 (2005).
[20]L. Wang, P. P. Ho, X. Liang, H. Dai, and R. R. Alfano, Opt. Lett. **18**, 241 (1993).
[21]M. Rahm, M. Paciaroni, Z. Wang, D. Sedarsky, and M. Linne, Opt. Express **23**, 22444 (2015).
[22]Y. Ren, J. Si, W. Tan, S. Xu, J. Tong, and X. Hou, IEEE Photonics Technol. Lett. **28**, 394 (2016).
[23]Q. Zhong and J. T. Fourkas, J. Chem. Phys. **112**, 15529 (2008).
[24]M. Paciaroni and M. Line, Appl. Opt. **43**, 5100 (2004).
[25]Lord Rayleigh, Philos. Mag. Ser. 5 **8**, 261 (1879).
[26]B. Redding, M. A. Choma, and H. Cao, Nat. Photonics **6**, 355 (2012).
[27]S. Idlahcen, L. Méès, C. Rozé, T. Girasole, and J. B. Blaisot, J. Opt. Soc. Am. A **26**, 1995 (2009).
[28]F. Mathieu, M. A. Reddemann, J. Palmer, and R. Kneer, Opt. Express **22**, 7058 (2014).
[29]J. B. Schmidt, Z. D. Schaefer, T. R. Meyer, S. Roy, S. A. Danczyk, and R. Gord, Appl. Opt. **48**, B137 (2009).